Wiley
Journal of Engineering
Volume 2025, Article ID 5524853, 16 pages
https://doi.org/10.1155/je/5524853

WILEY

Research Article

Comparative Study of Hybrid Control Using VTLCD and UTLCD for Building Models Subjected to Earthquake Loads

Ngoc-An Tran[1], **Hai-Le Bui**[2], **and Huong Quoc Cao**[3]

[1]*Faculty of Civil Engineering, Vietnam Maritime University, Haiphong City, Vietnam*
[2]*School of Mechanical Engineering, Hanoi University of Science & Technology, Hanoi, Vietnam*
[3]*School of Mechanical and Mechatronic Engineering, Faculty of Engineering and Information Technology, University of Technology Sydney, Sydney, New South Wales, Australia*

Correspondence should be addressed to Hai-Le Bui; le.buihai@hust.edu.vn

Received 20 March 2025; Revised 23 July 2025; Accepted 4 August 2025

Academic Editor: Arpan Hazra

Our previous study presented the vibration reduction efficiency of building models equipped with the V-shaped tuned liquid column damper (VTLCD) subjected to earthquake loads as a passive control problem. This study develops a hybrid control problem for VTLCD. The VTLCD is installed on the structure's top floor, and the control force is placed on the structure's first floor. The controller used to calculate this control force is based on the hedge-algebras (HA) theory, an advanced approach in automatic control. A U-shaped tuned liquid column damper (UTLCD) has also been included for comparison with VTLCD. The advantages of VTLCD over UTLCD were demonstrated in our previous research on the passive control problem and are further shown in this study on the hybrid control problem. Simulation results in this research show that the hybrid control configuration using VTLCD is significantly better at reducing structural vibrations than the one using UTLCD in all investigated earthquakes with different peak ground accelerations (PGAs). This efficiency increases as the PGA of the investigated earthquakes increases, demonstrating the advantage of VTLCD even in the case of hybrid control. This study has shown the potential of VTLCD as an effective solution to vibration control problems of structures.

Keywords: buildings subjected to earthquakes; hedge algebras; hybrid control; optimization; UTLCD; VTLCD

1. Introduction

Due to their slender structure, civil engineering structures such as high-rise buildings and large-span bridges are susceptible to dynamic loads (earthquakes, winds, etc.) [1, 2]. These vibrations can affect the strength and stability of the structure, as well as human health and safety. Therefore, developing methods to reduce vibrations in construction structures has received the attention of many researchers. Some types of mass-damping devices applied to construction structures include tuned mass damper (TMD) [3], tuned liquid damper (TLD) [4], and tuned liquid column damper (TLCD) [5].

TMDs are a prevalent type of damping device, applied not only to the construction field but also to mechanical engineering, aviation, power transmission, etc. For high-rise buildings, TMDs have been researched and used in both active and passive controls, for example, for buildings subjected to wind loads [6–8] or earthquake loads [9, 10]. TMDs were also widely studied and used for long-span bridges subjected to dynamic loads from the environment [11, 12]. TMDs are often optimally designed [13, 14], used in multi-TMD configurations [15], or supplemented with additional components [16] when applied to structural applications. Another type of mass-damping device of interest is the TLD. A TLD has a simple structure, including a cylindrical or rectangular liquid container. A TLD can be modeled as an equivalent TMD. The vibration and damping of the fluid during motion are comparable to the vibration of the mass and the damping in TMDs. TLDs are also commonly used

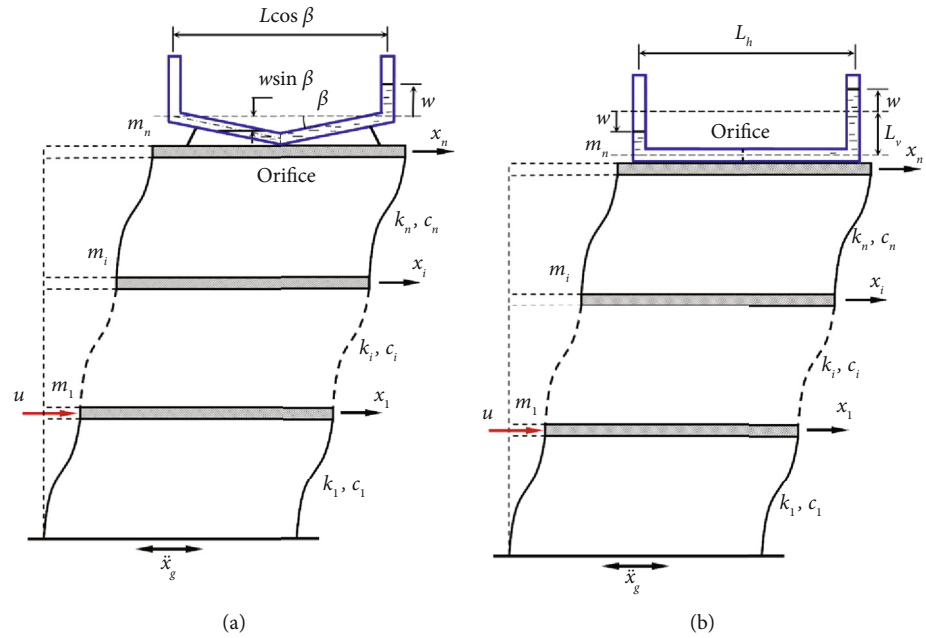

Figure 1: The hybrid control model with (a) VTLCD or (b) UTLCD.

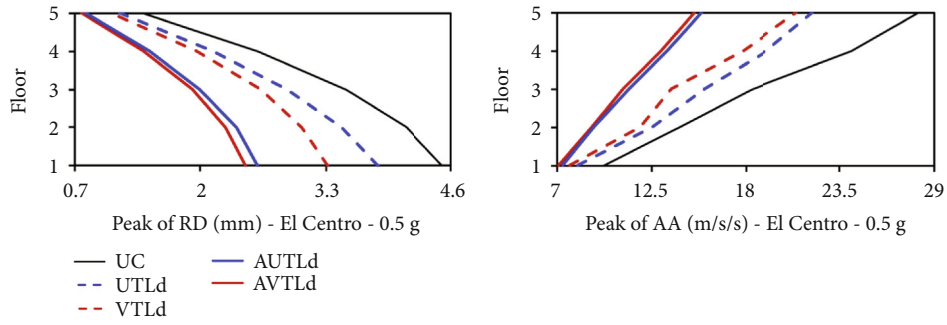

Figure 2: Peak of RD and AA of the structure, El Centro—0.5 g.

for structures subjected to wind [17, 18] or earthquake [19, 20] loads. Moreover, improved forms of TLDs, such as deep tank dampers [21–23] and overhead water tanks [24], have also been developed for building vibration reduction and fire suppression.

In addition to the dampers mentioned above, TLCD has also received attention from many studies. Research on the effectiveness of different control algorithms for semiactive control of TLCD applied to multidegree-of-freedom structures subjected to harmonic and random excitation was presented in [25]. In [26], TLCD was used to reduce vibrations for a 76-story building subjected to wind. The potential of TLCDs for mitigating seismic responses in short-period structures was investigated in [27], where their effectiveness under various ground motions was demonstrated. In [28], a new model of semiactive TLCD was proposed, in which the TLCD was connected to the structure by a spring and damper. The authors in [29] analyzed the performance of TLCD in vibration control of multidegree of freedom (DOF) structures subjected to earthquake excitation through real-time hybrid simulation, considering the interaction between the ground and structure. Semiactive TLCD with an on-off damping controller for vibration control of buildings has been studied in [30]. The studies in [31] introduced a variant of TLCD called Upgraded-TLCD, and the numerical simulation results showed the effectiveness of the proposed device. The authors in [32, 33] developed an upgraded TLCD device for use in high-rise buildings subjected to earthquake loads with active and hybrid control.

VTLCD, an upgraded form of traditional UTLCD, was proposed in [34–36]. In this context, the parameters of UTLCDs and VTLCDs are optimized to reduce vibrations for one-DOF structures subjected to harmonic excitation [34, 35]. In [36], VTLCD was applied for passive control of the vibration of a floating wind turbine. A comparative study on the vibration reduction effectiveness between VTLCD and UTLCD (with the same mass) for a multistorey building model subjected to earthquake loads was proposed in [37]. Simulations in [37] showed outstanding advantages of VTLCD compared to UTLCD in passive control problems, such as being more

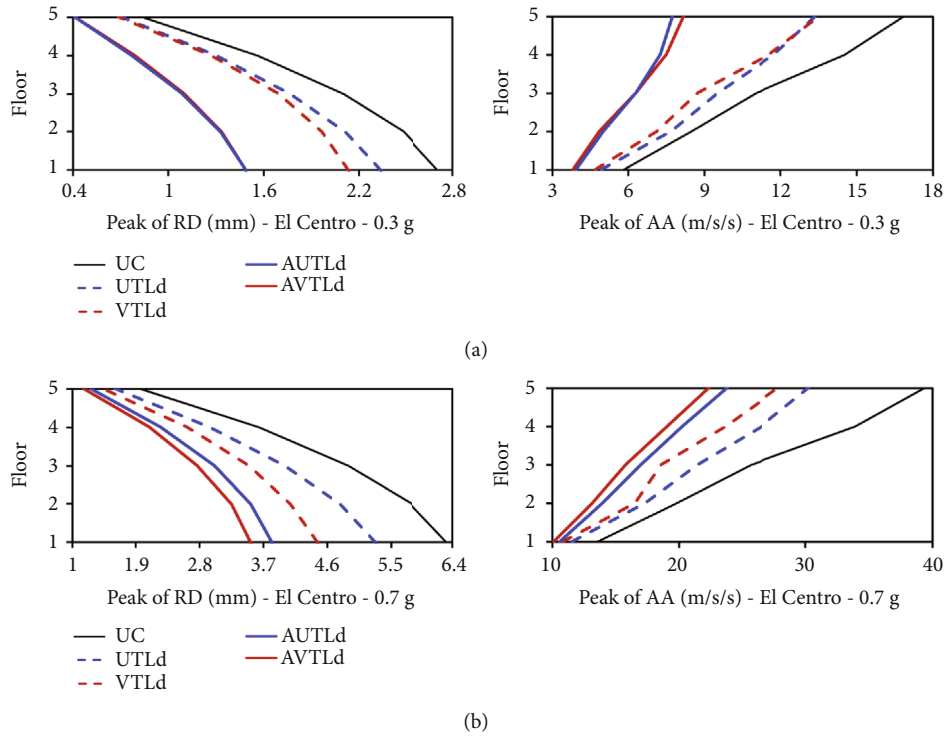

Figure 3: Peak of RD and AA of the structure (El Centro): (a) PGA = 0.3 g and (b) PGA = 0.7 g.

compact and having higher vibration reduction efficiency, especially for high peak ground acceleration earthquakes.

Hedge-algebras–based controllers (HACs) have been developed in several theoretical and experimental studies for mechanical models. Recent typical studies using HAC include the active control of building models subjected to earthquake loads [38, 39], the vibration reduction in active suspension systems [40, 41], and the motion control of mobile robots [42, 43]. Like controllers based on fuzzy set theory (FCs), HACs also use a qualitative rule system based on expert experience. The most significant difference between these controllers is the modeling of linguistic values of language variables. Linguistic values in HACs are represented by their fuzziness measure (a real number between 0 and 1), while they are fuzzy sets in FCs. This method of modeling linguistic values gives HACs many advantages compared to FCs, such as a more explicit and straightforward setup, higher control efficiency, easier optimization, and significantly faster calculation time to calculate control actions [43].

From the above analysis, this work presents a comparative study of hybrid control using VTLCD and UTLCD for building models subjected to earthquake loads, in which the parameters of the damping devices have been optimized to minimize the structure's peak relative displacement (RD). The contributions of this research are as follows.

- Developed an advanced hybrid control system for VTLCD to reduce vibrations for structures subjected to earthquake loads.
- Extended and confirmed the superior advantages of VTLCD compared to UTLCD in terms of the passive control problem and the hybrid control problem.
- Applied hedge algebra theory to control design to improve vibration reduction efficiency for structures subjected to earthquake loads.

2. Problem Under Consideration

Figure 1 presents an n-floor building model moving under the effect of earthquake load with ground acceleration $\ddot{x}_g$ [44]. The top floor of the building is fitted with VTLCD (Figure 1a) or UTLCD (Figure 1b). Also, the system includes a controlled force u on the first floor. The density of liquid moving in tubes is ρ. For the VTLCD in the static state, the liquid is only in the V-section, with a total liquid column length of L (two vertical branches do not contain liquid), and the cross-sectional area of the pipe branches is A_V. For UTLCD, also in the static state, the liquid columns in the vertical and horizontal components are L_v and L_h, respectively, and the cross-sectional area of the tube branches is A_U. For the convenience of comparison, this study only considers VTLCD and UTLCD with constant cross-sections and rectangular shapes. The head-loss coefficient of VTLCD is denoted by η_V, and that of UTLCD is denoted by η_U. The floor's concentrated masses are m_i, $i = [1, n]$. The system's generalized coordinates, containing the time-dependent variables, are $\mathbf{q} = [x_1, x_2, \cdots, x_n, w]^T$.

Using the transformation process as in [37] and with the controlled force u applied to the first floor, the motion equations of the system have the following form:

$$\begin{aligned}
&m_1\ddot{x}_1 + (c_1 + c_2)\dot{x}_1 - c_2\dot{x}_2 + (k_1 + k_2)x_1 - k_2x_2 = f_1 + u\\
&m_i\ddot{x}_i - c_i\dot{x}_{i-1} + (c_i + c_{i+1})\dot{x}_i - c_{i+1}\dot{x}_{i+1} - k_ix_{i-1} + (k_i + k_{i+1})x_i - k_{i+1}x_{i+1} = f_i\\
&(m_n + \mu_V L)\ddot{x}_n + \mu_V(L - |w|)\cos\beta\ddot{w} - c_n\dot{x}_{n-1} + c_n\dot{x}_n - k_nx_{n-1} + k_nx_n - \mu_V\cos\beta\dot{w}^2 = f_n\\
&\mu_V(L - |w|)\cos\beta\ddot{x}_n + \mu_V L\ddot{w} + 0.5\mu_V\eta_V|\dot{w}|\dot{w} + \mu_V g(1 + \sin\beta)w = (L - |w|)f_{n+1}.
\end{aligned} \tag{1}$$

In which $f_i = -m_i\ddot{x}_g$, $i = [2, n-1]$; $f_n = -(m_n + \mu_V L)\ddot{x}_g$; $f_{n+1} = -\mu_V\cos\beta\ddot{x}_g$. The ground acceleration $\ddot{x}_g$ and thus f_i, $i = [2, n+1]$, are also the time-dependent variables.

Similarly, when the structure uses UTLCD on the top floor, the system's state equations are as follows:

$$\begin{aligned}
&m_1\ddot{x}_1 + (c_1 + c_2)\dot{x}_1 - c_2\dot{x}_2 + (k_1 + k_2)x_1 - k_2x_2 = f_1 + u\\
&m_i\ddot{x}_i - c_i\dot{x}_{i-1} + (c_i + c_{i+1})\dot{x}_i - c_{i+1}\dot{x}_{i+1} - k_ix_{i-1} + (k_i + k_{i+1})x_i - k_{i+1}x_{i+1} = f_i\\
&(m_n + \mu_U L_e)\ddot{x}_n + \mu_U L_h\ddot{w} - c_n\dot{x}_{n-1} + c_n\dot{x}_n - k_nx_{n-1} + k_nx_n = f_n\\
&\mu_U L_h\ddot{x}_n + \mu_U L_e\ddot{w} + 0.5\mu_U\eta_U\dot{w}|\dot{w}| + 2\mu_U gw = f_{n+1},
\end{aligned} \tag{2}$$

where $\mu_U = A_U\rho$; $L_e = 2L_v + L_h$; $f_i = -m_i\ddot{x}_g$, $i = [2, n-1]$; $f_n = -(m_n + \mu_U L_e)\ddot{x}_g$; $f_{n+1} = -\mu_U L_h\ddot{x}_g$.

Equations (1) and (2) are written in matrix form as follows:

$$\begin{aligned}
&[M]\{\ddot{x}\} + [C]\{\dot{x}\} + [K]\{x\} = -[m]\{\ddot{x}_g\} + \{U\}\\
&\{x\} = \{x_1 \quad x_2 \quad \cdots \quad x_{n-1} \quad x_n \quad w\}^T\\
&\{U\} = \{u \quad 0 \quad \cdots \quad 0 \quad 0 \quad 0\}^T
\end{aligned} \tag{3}$$

The matrices $[M]$, $[C]$, $[K]$, and $[m]$ for the structure-VTLCD system are, respectively:

$$[M] = \begin{bmatrix}
m_1 & 0 & \cdots & 0 & 0 & 0\\
0 & m_2 & \cdots & 0 & 0 & 0\\
\cdots & \cdots & \cdots & \cdots & \cdots & \cdots\\
0 & 0 & \cdots & m_{n-1} & 0 & 0\\
0 & 0 & \cdots & 0 & m_n + \mu_V L & \mu_V(L - |w|)\cos\beta\\
0 & 0 & \cdots & 0 & \mu_V(L - |w|)\cos\beta & \mu_V L
\end{bmatrix},$$

$$[C] = \begin{bmatrix}
c_1 + c_2 & -c_2 & \cdots & 0 & 0 & 0\\
-c_2 & c_2 + c_3 & \cdots & 0 & 0 & 0\\
\cdots & \cdots & \cdots & \cdots & \cdots & \cdots\\
0 & 0 & \cdots & c_{n-1} + c_n & -c_n & 0\\
0 & 0 & \cdots & -c_n & c_n & -\mu_V\cos\beta\dot{w}\\
0 & 0 & \cdots & 0 & 0 & 0.5\mu_V\eta_V|\dot{w}|
\end{bmatrix},$$

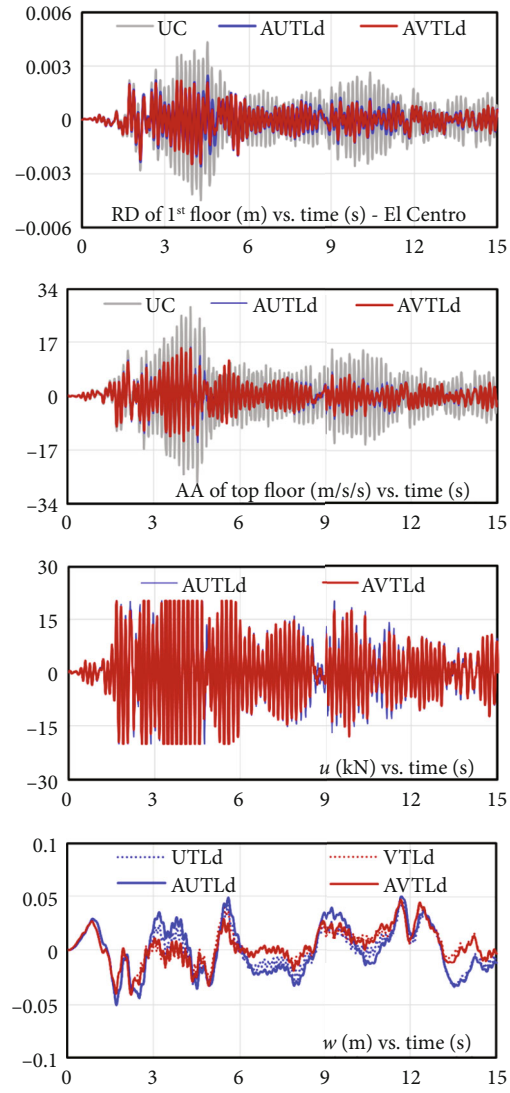

Figure 4: The system's time responses when PGA = 0.5 g.

$$[K] = \begin{bmatrix}
k_1 + k_2 & -k_2 & \cdots & 0 & 0 & 0\\
-k_2 & k_2 + k_3 & \cdots & 0 & 0 & 0\\
\cdots & \cdots & \cdots & \cdots & \cdots & \cdots\\
0 & 0 & \cdots & k_{n-1} + k_n & -k_n & 0\\
0 & 0 & \cdots & -k_n & k_n & 0\\
0 & 0 & \cdots & 0 & 0 & \mu_V g(1 + \sin\beta)
\end{bmatrix},$$

$$[m] = \begin{bmatrix}
m_1 & 0 & \cdots & 0 & 0 & 0\\
0 & m_2 & \cdots & 0 & 0 & 0\\
\cdots & \cdots & \cdots & \cdots & \cdots & \cdots\\
0 & 0 & \cdots & m_{n-1} & 0 & 0\\
0 & 0 & \cdots & 0 & m_n + \mu_V L & 0\\
0 & 0 & \cdots & 0 & \mu_V(L - |w|)\cos\beta & 0
\end{bmatrix}. \tag{4}$$

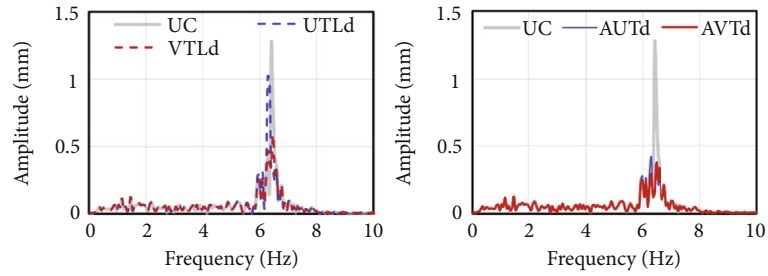

(a) Peak RD of the 1st floor, El Centro—0.5g

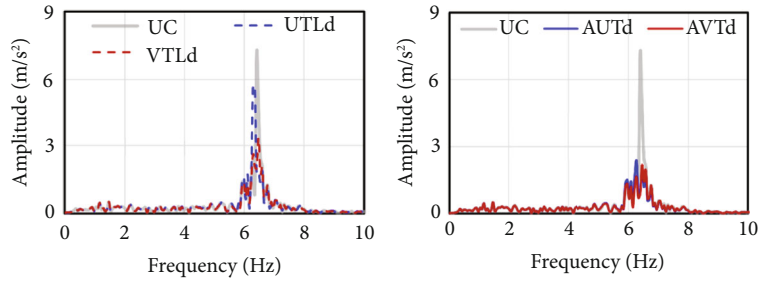

(b) Peak AA of the top floor, El Centro—0.5g

FIGURE 5: Frequency spectra of the 1st floor's peak RD and the top floor's peak AA, El Centro—0.5 g.

For the structure-UTLCD system, the matrices $[M]$, $[C]$, $[K]$, and $[m]$ are, respectively,

$$[M] = \begin{bmatrix} m_1 & 0 & \cdots & 0 & 0 & 0 \\ 0 & m_2 & \cdots & 0 & 0 & 0 \\ \cdots & \cdots & \cdots & \cdots & \cdots & \cdots \\ 0 & 0 & \cdots & m_{n-1} & 0 & 0 \\ 0 & 0 & \cdots & 0 & m_n + \mu_U L_e & \mu_U L_h \\ 0 & 0 & \cdots & 0 & \mu_U L_h & \mu_U L_e \end{bmatrix},$$

$$[C] = \begin{bmatrix} c_1 + c_2 & -c_2 & \cdots & 0 & 0 & 0 \\ -c_2 & c_2 + c_3 & \cdots & 0 & 0 & 0 \\ \cdots & \cdots & \cdots & \cdots & \cdots & \cdots \\ 0 & 0 & \cdots & c_{n-1} + c_n & -c_n & 0 \\ 0 & 0 & \cdots & -c_n & c_n & 0 \\ 0 & 0 & \cdots & 0 & 0 & 0.5\mu_U \eta_U |\dot{w}| \end{bmatrix},$$

$$[K] = \begin{bmatrix} k_1 + k_2 & -k_2 & \cdots & 0 & 0 & 0 \\ -k_2 & k_2 + k_3 & \cdots & 0 & 0 & 0 \\ \cdots & \cdots & \cdots & \cdots & \cdots & \cdots \\ 0 & 0 & \cdots & k_{n-1} + k_n & -k_n & 0 \\ 0 & 0 & \cdots & -k_n & k_n & 0 \\ 0 & 0 & \cdots & 0 & 0 & 2\mu_U g \end{bmatrix},$$

$$[m] = \begin{bmatrix} m_1 & 0 & \cdots & 0 & 0 & 0 \\ 0 & m_2 & \cdots & 0 & 0 & 0 \\ \cdots & \cdots & \cdots & \cdots & \cdots & \cdots \\ 0 & 0 & \cdots & m_{n-1} & 0 & 0 \\ 0 & 0 & \cdots & 0 & m_n + \mu_U L_e & 0 \\ 0 & 0 & \cdots & 0 & \mu_U L_h & 0 \end{bmatrix}. \quad (5)$$

The 4th-order Runge–Kutta method [45] is used to solve nonlinear differential equations in Equations (1) and (2).

As presented in [37], the following criteria need to be minimized:

$$C_D = \max_{i=1:n} \left(\frac{\max |d_i|}{\max |d_{i,\mathrm{UC}}|} \right), \quad (6)$$

$$C_A = \max_{i=1:n} \left(\frac{\max |a_i|}{\max |a_{i,\mathrm{UC}}|} \right). \quad (7)$$

Equation (6), corresponding to the maximum RD C_D, is used to evaluate structural safety, and Equation (7), corresponding to the maximum absolute acceleration (AA) C_A, is used to assess human safety. In which d_i and a_i are the peak RD and AA of the i^{th} floor, respectively. The notation "UC" (uncontrolled case) means the main structure does not have additional damping devices and control forces.

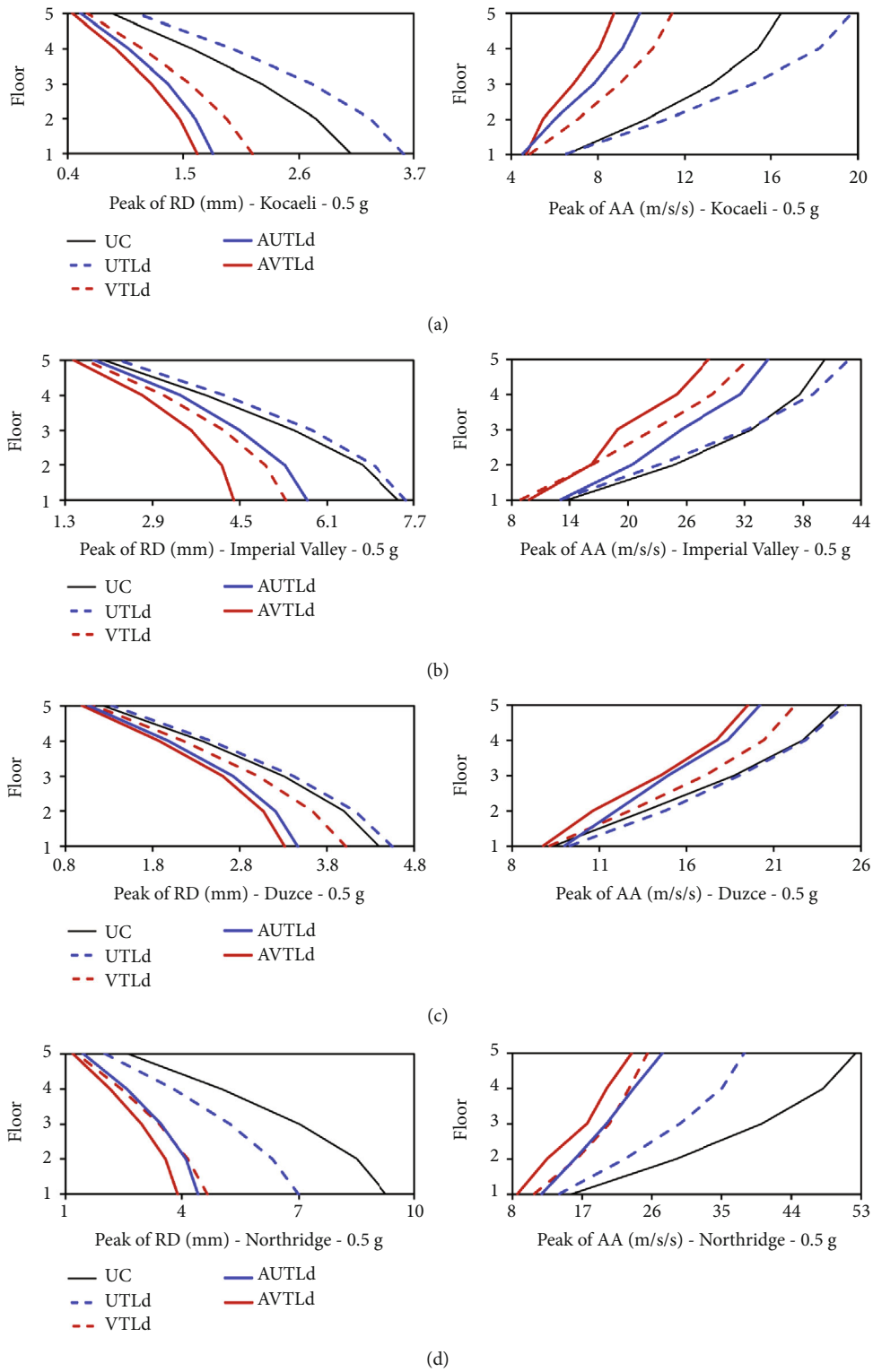

Figure 6: Continued.

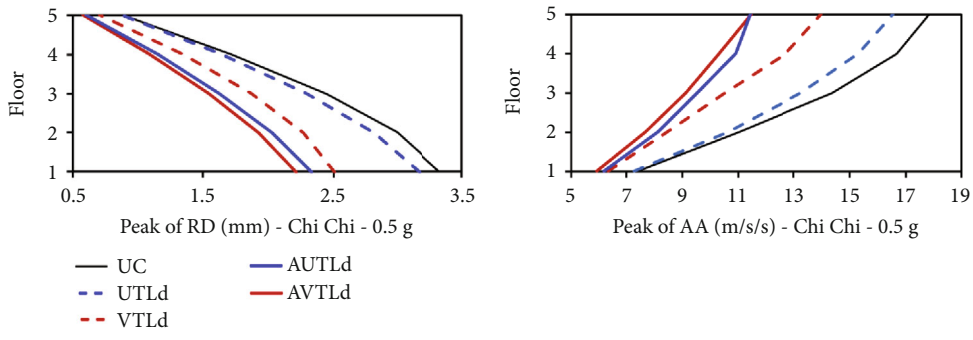

(e)

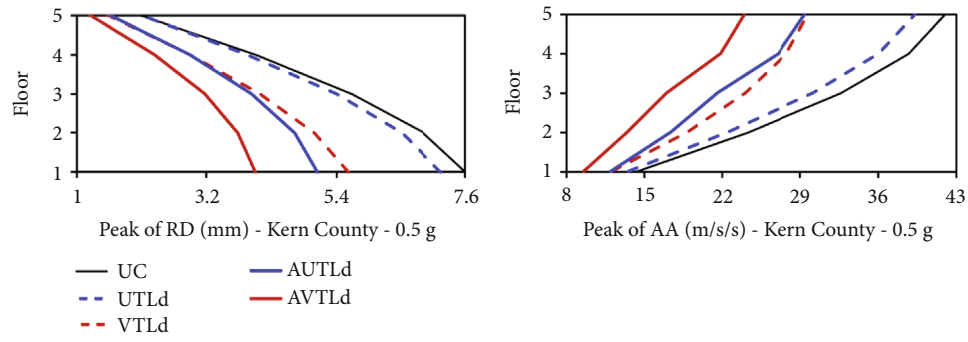

(f)

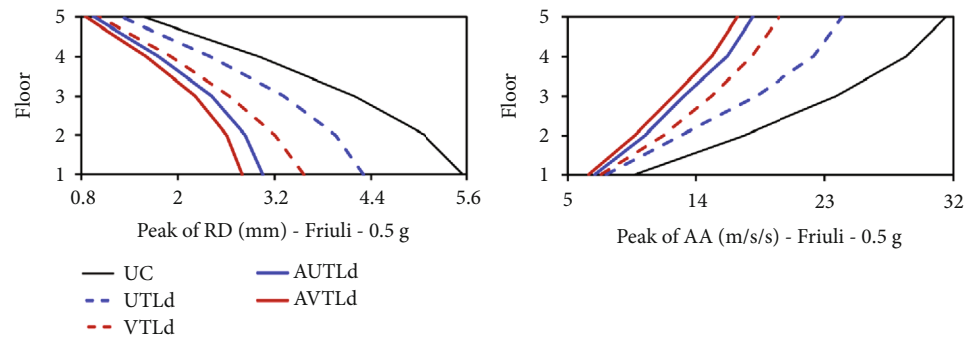

(g)

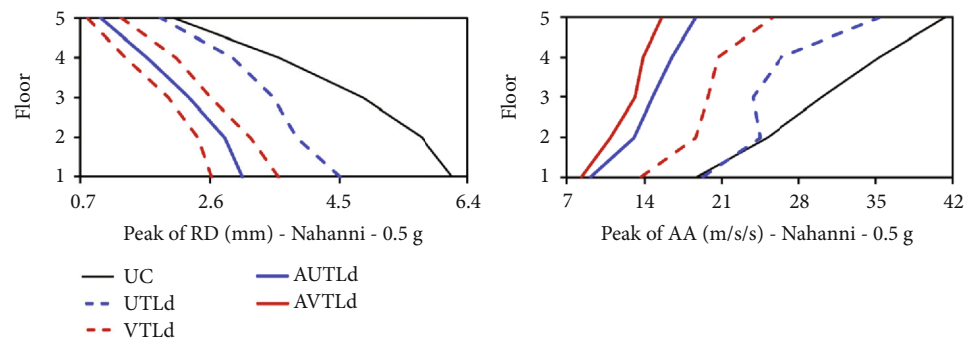

(h)

Figure 6: Continued.

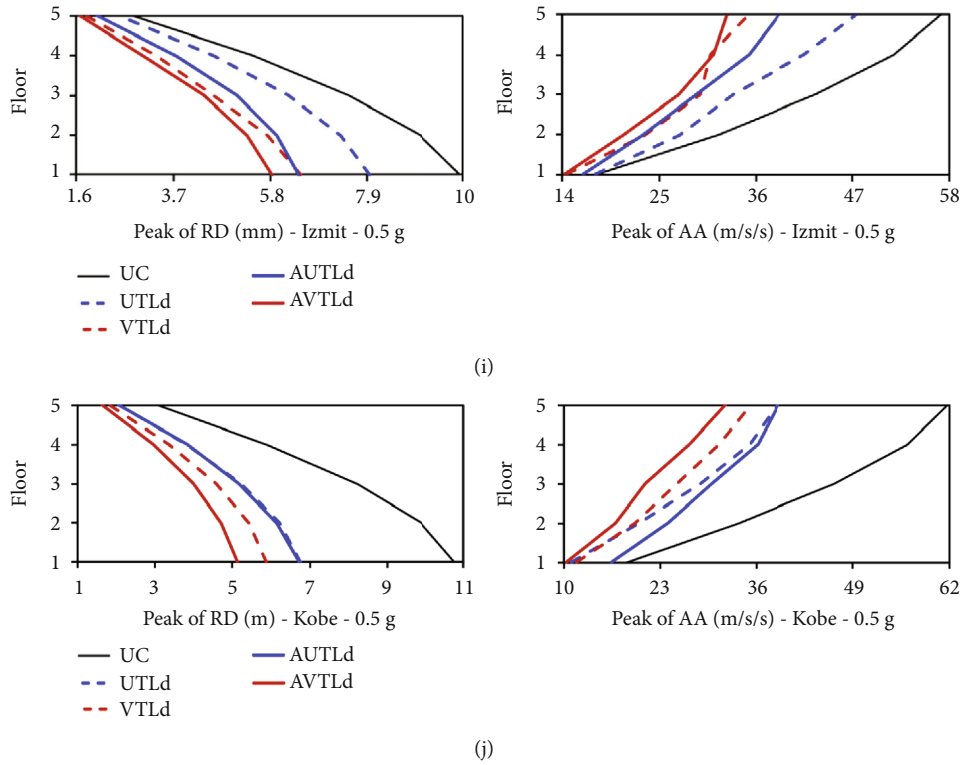

Figure 6: (a–j) Peak of RD and AA of the structure's floors, 10 testing earthquakes – 0.5 g.

3. HAC

The hedge-algebras theory was proposed in 1990 [46, 47]. It is a powerful tool for modeling linguistic values of linguistic variables. The main features of the HA theory include the following: the natural semantic order of linguistic values is always guaranteed, and the fuzziness measure of linguistic values is represented by real numbers from 0 to 1 [48]. Because of such representation, using fuzzy sets to describe linguistic values is unnecessary, as in fuzzy set theory. The HA theory has been effectively applied to the problems of information technology and control [49].

A controller based on the HA theory (HAC) has the same operating principle as a fuzzy set theory-based controller (FC). The operation of components in HAC is straightforward through linear interpolation steps. Therefore, the computation time of HACs is much faster than that of FCs [43]. The research results in [38] have demonstrated that an explicit equation can express the relationship between control and state variables when choosing the appropriate control rule base and linguistic values for state and control variables.

For the active control problem in this study, using the explicit formula of HAC in [38], the control force u is determined through the state variables x_1 and $\dot{x}_1$ as follows:

$$u = \frac{2c}{3a}x_1 + \frac{c}{3b}\dot{x}_1, \tag{8}$$

where a, b, and c are the boundary values of the reference range of the variables x_1, $\dot{x}_1$, and u, respectively.

4. Numerical Simulations

The five-floor building structure ($n = 5$) in [37] is recalled with the following parameters: $m_i = 10 \times 10^3$ kg, $c_i = 8 \times 10^3$ Ns/m, and $k_i = 200 \times 10^6$ N/m, $i = [1 : n]$. In this study, a, b, and c values are selected as 5 m, 1 m/s, and 1200 kN through a trial-and-error step. The maximum control force is $u_{\max} = 20$ kN.

Simulation results in [37] have shown that the configuration of the VTLCD optimized according to the RD criterion (Equation 6) is more effective than the VTLCD optimized following the AA criterion (Equation 7). Therefore, the simulation in this study will focus on comparing the passive cases of UTLCD and VTLCD optimized according to the RD of the structure in [37] (denoted by UTLd and VTLd, respectively) with the system with additional active control force u (denoted by AUTLd and AVTLd, respectively). It should be noted that the simulation results for the UTLd and VTLd cases are extracted from [37].

The range for optimal selection of the parameters of VTLd and UTLd is as follows [37]:

$$L(\mathrm{m}) \in [2, 10], bV(\mathrm{m}) \in [0.2, 2], hV(\mathrm{m}) \in [0.2, 2]\, \beta(^\circ) \in [5, 60]\eta_V \in [0, 300],$$
$$L_h(\mathrm{m}) \in [2, 10], Lv(\mathrm{m}) \in [0.1, 2], b_U(\mathrm{m}) \in [0.2, 2], h_U(\mathrm{m}) \in [0.2, 2], \eta_U \in [0, 300]. \tag{9}$$

TABLE 1: C_D, C_A, and $w_{\max}$ (PGA = 0.7 g).

Earthquake	Criterion	VTLd	UTLd	Variation (%)	AVTLd	AUTLd	Variation (%)
El Centro	C_D	0.708	0.838	−15.53	0.558	0.607	−8.07
	C_A	0.711	0.771	−7.78	0.568	0.606	−6.15
	$W_{\max}$, m	0.058	0.063	−8.16	0.058	0.067	−14.20
Kocaeli	C_D	0.677	1.137	−40.47	0.537	0.605	−11.17
	C_A	0.672	1.171	−42.60	0.574	0.666	−13.82
	$W_{\max}$, m	0.129	0.188	−31.31	0.152	0.225	−32.43
Imperial Valley	C_D	0.725	0.981	−26.08	0.621	0.814	−23.68
	C_A	0.786	1.011	−22.24	0.713	0.879	−18.90
	$W_{\max}$, m	0.029	0.038	−25.24	0.032	0.041	−22.38
Duzce	C_D	0.907	1.026	−11.60	0.766	0.802	−4.45
	C_A	0.873	1.005	−13.12	0.800	0.839	−4.64
	$W_{\max}$, m	0.055	0.076	−27.32	0.057	0.074	−23.47
Northridge	C_D	0.497	0.725	−31.39	0.433	0.493	−12.15
	C_A	0.473	0.699	−32.31	0.458	0.545	−15.94
	$W_{\max}$, m	0.047	0.063	−26.08	0.049	0.064	−23.17
Chi-Chi	C_D	0.720	0.939	−23.28	0.675	0.722	−6.49
	C_A	0.745	0.915	−18.57	0.635	0.670	−5.35
	$W_{\max}$, m	0.081	0.114	−28.56	0.089	0.145	−38.39
Kern County	C_D	0.724	0.926	−21.88	0.564	0.721	−21.79
	C_A	0.675	0.918	−26.43	0.575	0.747	−23.09
	$W_{\max}$, m	0.074	0.099	−25.84	0.074	0.099	−25.38
Friuli	C_D	0.619	0.756	−18.09	0.512	0.565	−9.39
	C_A	0.601	0.753	−20.26	0.525	0.574	−8.49
	$W_{\max}$, m	0.038	0.044	−13.35	0.039	0.045	−12.95
Nahanni	C_D	0.565	0.701	−19.51	0.446	0.535	−16.62
	C_A	0.590	0.829	−28.81	0.401	0.531	−24.55
	$W_{\max}$, m	0.015	0.018	−13.46	0.014	0.018	−20.13
Izmit	C_D	0.655	0.769	−14.87	0.605	0.668	−9.43
	C_A	0.600	0.811	−25.97	0.557	0.694	−19.75
	$W_{\max}$, m	0.115	0.136	−15.17	0.114	0.132	−13.43
Kobe	C_D	0.546	0.624	−12.48	0.491	0.635	−22.67
	C_A	0.554	0.629	−11.99	0.507	0.630	−19.58
	$W_{\max}$, m	0.043	0.073	−41.20	0.056	0.096	−41.44

The optimal parameters of VTLd and UTLd are as follows [37]:

$$[L(\mathrm{m})\ b_V(\mathrm{m}) h_V(\mathrm{m})\ \beta(^\circ)\eta_V] = [2.383 \quad 0.899 \quad 0.467 \quad 5.634 \quad 300],$$
$$[L_h(\mathrm{m})\ L_v(\mathrm{m}) b_U(\mathrm{m})\ h_U(m)\eta_U] = [5.092 \quad 1.271 \quad 0.376 \quad 0.348 \quad 300]. \tag{10}$$

First, the peaks RD and AA of floors are shown in Figure 2 for the El Centro earthquake with its PGA equal to 0.5 g. The results in Figure 2 show that AVTLd and AUTLd are significantly more effective than VTLd and UTLd. AVTLd and AUTLd reduction ratios are 45% and 42% for the RD of the first floor and 46% and 45% for the AA of the top floor, respectively. Figure 3 shows the peak RD and AA of floors for the El Centro earthquake with its PGA equal to 0.3 and 0.7 g. Like the passive control cases for the El Centro earthquake [37], when PGA = 0.3 g, the damping efficiency of AVTLd and AUTLd has a reduced difference compared to the case of PGA = 0.5 g; and vice versa when PGA = 0.7 g. This effect is clearly represented in Figure 3. Figure 4

TABLE 2: RMS value of criteria (PGA = 0.7 g).

Earthquake	Criterion	VTLd	UTLd	Variation (%)	AVTLd	AUTLd	Variation (%)
El Centro	x_1, mm	0.010	0.013	−27.23	0.008	0.008	−7.15
	$\ddot{x}_5$, m/s^2	0.055	0.075	−26.81	0.043	0.046	−6.68
	w, mm	0.173	0.187	−7.40	0.171	0.225	−23.87
	u, kN	0.102	0.125	−18.59	0.090	0.096	−5.86
Kocaeli	x_1, mm	0.009	0.015	−37.05	0.006	0.007	−8.47
	$\ddot{x}_5$, m/s^2	0.050	0.081	−38.19	0.033	0.036	−9.33
	w, mm	0.574	0.817	−29.80	0.611	0.882	−30.74
	u, kN	0.115	0.131	−12.16	0.079	0.085	−7.19
Imperial Valley	x_1, mm	0.019	0.033	−41.71	0.014	0.021	−32.75
	$\ddot{x}_5$, m/s^2	0.108	0.184	−41.34	0.081	0.120	−32.57
	w, mm	0.090	0.118	−23.50	0.093	0.114	−18.56
	u, kN	0.121	0.129	−6.57	0.104	0.122	−14.84
Duzce	x_1, mm	0.012	0.020	−38.32	0.009	0.011	−14.94
	$\ddot{x}_5$, m/s^2	0.067	0.110	−39.17	0.050	0.059	−16.10
	w, mm	0.145	0.217	−33.04	0.170	0.251	−32.08
	u, kN	0.118	0.129	−8.80	0.094	0.103	−9.26
Northridge	x_1, mm	0.019	0.024	−21.68	0.015	0.018	−16.81
	$\ddot{x}_5$, m/s^2	0.107	0.136	−21.37	0.082	0.099	−17.08
	w, mm	0.095	0.145	−34.20	0.113	0.154	−26.87
	u, kN	0.137	0.138	−0.30	0.120	0.128	−6.28
Chi-Chi	x_1, mm	0.009	0.011	−16.07	0.008	0.008	−2.80
	$\ddot{x}_5$, m/s^2	0.050	0.060	−16.57	0.039	0.040	−2.49
	w, mm	0.235	0.465	−49.61	0.290	0.533	−45.63
	u, kN	0.108	0.124	−12.46	0.091	0.093	−2.24
Kern County	x_1, mm	0.016	0.025	−33.86	0.012	0.016	−23.16
	$\ddot{x}_5$, m/s^2	0.091	0.137	−33.87	0.068	0.090	−23.86
	w, mm	0.188	0.214	−12.19	0.188	0.227	−17.11
	u, kN	0.126	0.146	−14.06	0.108	0.112	−3.55
Friuli	x_1, mm	0.013	0.021	−39.27	0.008	0.010	−19.12
	$\ddot{x}_5$, m/s^2	0.071	0.117	−39.12	0.045	0.056	−19.42
	w, mm	0.058	0.078	−25.25	0.060	0.077	−22.59
	u, kN	0.117	0.140	−16.69	0.083	0.094	−11.15
Nahanni	x_1, mm	0.014	0.020	−29.04	0.009	0.011	−21.40
	$\ddot{x}_5$, m/s^2	0.087	0.125	−30.30	0.054	0.068	−20.54
	w, mm	0.047	0.052	−10.01	0.039	0.047	−17.14
	u, kN	0.127	0.134	−4.97	0.104	0.110	−5.97
Izmit	x_1, mm	0.023	0.037	−38.47	0.018	0.026	−31.65
	$\ddot{x}_5$, m/s^2	0.127	0.206	−38.15	0.102	0.149	−31.54
	w, mm	0.736	0.883	−16.65	0.724	0.877	−17.46
	u, kN	0.125	0.138	−9.45	0.098	0.116	−15.02
Kobe	x_1, mm	0.024	0.031	−22.58	0.020	0.027	−25.05
	$\ddot{x}_5$, m/s^2	0.133	0.171	−22.18	0.113	0.151	−25.23
	w, mm	0.106	0.171	−38.35	0.142	0.226	−37.27
	u, kN	0.141	0.146	−3.67	0.127	0.141	−10.06

TABLE 3: C_D, C_A, and w_{max} (PGA = 0.3 g).

Earthquake	Criterion	VTLd	UTLd	Variation (%)	AVTLd	AUTLd	Variation (%)
El Centro	C_D	0.790	0.865	−8.67	0.550	0.550	−0.17
	C_A	0.804	0.794	1.20	0.485	0.459	5.47
	W_{max}, m	0.032	0.035	−10.81	0.034	0.035	−4.51
Kocaeli	C_D	0.742	1.200	−38.19	0.538	0.577	−6.77
	C_A	0.735	1.231	−40.29	0.536	0.586	−8.59
	W_{max}, m	0.079	0.107	−25.57	0.083	0.122	−31.35
Imperial Valley	C_D	0.757	1.103	−31.38	0.551	0.698	−21.11
	C_A	0.837	1.146	−26.95	0.664	0.803	−17.29
	W_{max}, m	0.020	0.025	−18.35	0.026	0.033	−20.58
Duzce	C_D	0.930	1.046	−11.10	0.753	0.783	−3.84
	C_A	0.924	1.020	−9.43	0.752	0.770	−2.37
	W_{max}, m	0.032	0.044	−28.37	0.035	0.048	−26.59
Northridge	C_D	0.529	0.794	−33.34	0.407	0.460	−11.59
	C_A	0.529	0.759	−30.33	0.426	0.488	−12.81
	W_{max}, m	0.030	0.034	−11.52	0.031	0.035	−13.21
Chi-Chi	C_D	0.801	0.963	−16.85	0.672	0.697	−3.59
	C_A	0.838	0.941	−10.96	0.632	0.640	−1.21
	W_{max}, m	0.051	0.085	−39.75	0.063	0.096	−34.97
Kern County	C_D	0.770	0.972	−20.74	0.495	0.582	−14.99
	C_A	0.770	0.960	−19.87	0.535	0.618	−13.49
	W_{max}, m	0.046	0.056	−17.55	0.046	0.056	−17.46
Friuli	C_D	0.682	0.800	−14.81	0.498	0.533	−6.59
	C_A	0.695	0.795	−12.64	0.502	0.538	−6.67
	W_{max}, m	0.023	0.025	−8.44	0.023	0.025	−8.21
Nahanni	C_D	0.615	0.767	−19.81	0.411	0.453	−9.24
	C_A	0.669	0.888	−24.68	0.347	0.367	−5.43
	W_{max}, m	0.008	0.009	−7.67	0.007	0.010	−23.52
Izmit	C_D	0.653	0.855	−23.63	0.567	0.613	−7.54
	C_A	0.647	0.873	−25.90	0.571	0.637	−10.46
	W_{max}, m	0.054	0.065	−18.00	0.052	0.066	−20.82
Kobe	C_D	0.577	0.632	−8.76	0.456	0.564	−19.14
	C_A	0.607	0.627	−3.19	0.495	0.606	−18.42
	W_{max}, m	0.026	0.041	−36.18	0.033	0.045	−27.24

illustrates the time responses of the RD of the first floor, the AA of the top floor, the liquid displacement w, and the control force u when PGA = 0.5 g. Hence, the time response of displacement of the liquid column w in the cases of VTLd, UTLd, AVTLd, and AUTLd is not very different.

The fast Fourier transform (FFT) [50] is used to investigate the frequency spectra of the 1st floor's peak RD and the top floor's peak AA with the PGA of 0.5 g in different damper configurations for the El Centro earthquake, as shown in Figure 5a,b, respectively.

The above simulation results are for the case of the El Centro earthquake. Next, investigations of 10 other earthquakes (including Kocaeli, Imperial Valley, Duzce, Northridge, Chi-Chi, Kern County, Friuli, Nahanni, Izmit, and Kobe earthquakes) are performed to validate the stability of the hybrid control configurations. These earthquakes are commonly investigated in studies of earthquake-resistant structures [51–53]. In addition, the effectiveness of passive VTLCD and UTLCD has been verified through these earthquakes [37]. Therefore, they are included in this study to facilitate comparison between passive and hybrid

TABLE 4: RMS value of criteria (PGA = 0.3 g).

Earthquake	Criterion	VTLd	UTLd	Variation (%)	AVTLd	AUTLd	Variation (%)
El Centro	x_1, mm	0.005	0.006	−23.64	0.003	0.004	−4.49
	$\ddot{x}_5$, m/s^2	0.026	0.033	−22.53	0.018	0.019	−3.67
	w, mm	0.097	0.126	−23.37	0.100	0.147	−31.49
	u, kN	0.065	0.089	−26.58	0.050	0.052	−4.21
Kocaeli	x_1, mm	0.004	0.007	−36.89	0.003	0.003	−5.62
	$\ddot{x}_5$, m/s^2	0.023	0.038	−37.65	0.014	0.015	−5.68
	w, mm	0.316	0.448	−29.40	0.339	0.496	−31.67
	u, kN	0.064	0.095	−32.01	0.037	0.039	−6.83
Imperial Valley	x_1, mm	0.009	0.016	−43.85	0.006	0.007	−20.98
	$\ddot{x}_5$, m/s^2	0.051	0.090	−43.30	0.032	0.040	−20.33
	w, mm	0.053	0.063	−15.13	0.064	0.079	−19.25
	u, kN	0.102	0.119	−14.24	0.071	0.082	−13.16
Duzce	x_1, mm	0.006	0.009	−39.47	0.004	0.004	−7.01
	$\ddot{x}_5$, m/s^2	0.031	0.051	−40.01	0.021	0.022	−6.90
	w, mm	0.086	0.132	−35.12	0.110	0.163	−32.56
	u, kN	0.082	0.110	−25.78	0.053	0.057	−7.38
Northridge	x_1, mm	0.010	0.011	−13.47	0.006	0.006	−11.08
	$\ddot{x}_5$, m/s^2	0.056	0.064	−12.78	0.032	0.036	−10.77
	w, mm	0.062	0.087	−29.31	0.074	0.109	−32.45
	u, kN	0.118	0.113	4.09	0.082	0.087	−6.62
Chi-Chi	x_1, mm	0.004	0.005	−10.61	0.003	0.003	0.05
	$\ddot{x}_5$, m/s^2	0.024	0.026	−10.20	0.017	0.017	1.25
	w, mm	0.172	0.322	−46.60	0.212	0.348	−39.00
	u, kN	0.064	0.072	−11.25	0.044	0.044	1.38
Kern County	x_1, mm	0.008	0.011	−28.01	0.005	0.006	−12.22
	$\ddot{x}_5$, m/s^2	0.046	0.064	−27.57	0.027	0.031	−12.23
	w, mm	0.102	0.108	−5.24	0.101	0.127	−20.38
	u, kN	0.104	0.125	−17.02	0.068	0.074	−7.48
Friuli	x_1, mm	0.007	0.010	−32.52	0.003	0.003	−7.37
	$\ddot{x}_5$, m/s^2	0.038	0.056	−32.06	0.018	0.019	−6.92
	w, mm	0.036	0.044	−16.86	0.039	0.045	−14.94
	u, kN	0.096	0.124	−22.33	0.049	0.052	−6.95
Nahanni	x_1, mm	0.007	0.009	−19.76	0.004	0.004	−9.38
	$\ddot{x}_5$, m/s^2	0.045	0.059	−22.44	0.022	0.023	−7.69
	w, mm	0.027	0.027	0.27	0.023	0.026	−12.04
	u, kN	0.107	0.115	−7.01	0.059	0.064	−7.60
Izmit	x_1, mm	0.011	0.018	−41.37	0.007	0.009	−25.41
	$\ddot{x}_5$, m/s^2	0.061	0.104	−40.90	0.038	0.051	−25.13
	w, mm	0.331	0.373	−11.17	0.320	0.375	−14.59
	u, kN	0.109	0.130	−15.86	0.072	0.082	−13.04
Kobe	x_1, mm	0.011	0.014	−16.79	0.008	0.010	−19.87
	$\ddot{x}_5$, m/s^2	0.065	0.077	−16.00	0.044	0.054	−19.60
	w, mm	0.063	0.099	−36.17	0.090	0.119	−24.05
	u, kN	0.120	0.132	−9.19	0.094	0.104	−9.70

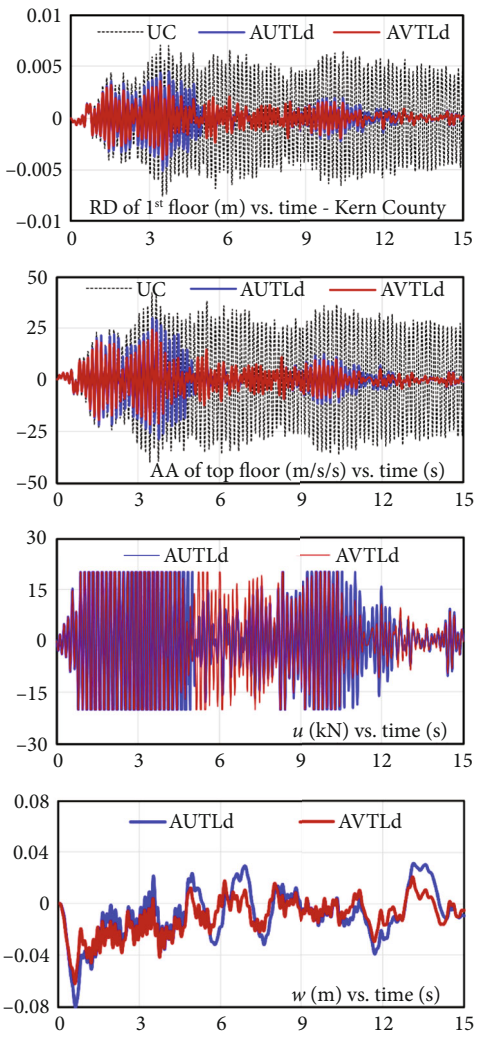

Figure 7: Time responses of the system, Kern County—0.5 g.

configurations of VTLCD and UTLCD. The investigated results of VTLd, UTLd, AVTLd, and AUTLd for 10 testing earthquakes (PGA = 0.5 g) are shown in Figure 6. C_D, C_A, the peak value of w (w_{max}), and the root mean square (RMS) values of essential criteria are listed in Tables 1, 2, 3, and 4. The column "variation, %" represents the percentage change in the results obtained with VTLd compared to UTLd or AVTLd compared to AUTLd.

The results presented in Figure 6 and Tables 1, 2, 3, and 4 for 10 testing earthquakes with different PGA values show that AVTLd has high damping efficiency. The highest reduction ratio of the RD of the first floor is 59% in the case of the Northridge earthquake, and the highest reduction ratio of the AA of the top floor is 65% in the case of the Nahanni earthquake, with all three different values of PGA. In all simulation results in Figure 6 and Tables 1, 2, 3, and 4, the efficiency of AVTLd is significantly higher than that of AUTLd with the same mass of liquid column, parameters of the HA theory-based controller, and maximum control force (20 kN). Even the efficiency of AUTLd is less than or equal to that of VTLd in cases of the Imperial Valley (0.5 and 0.7 g), Northridge (0.5 and 0.7 g), Kern County (0.7 g), Izmit (0.5 and 0.7 g), and Kobe (0.3, 0.5, and 0.7 g) earthquakes.

To better illustrate the vibration reduction effect of VTLCD and UTLCD in combination with an active controller based on the HA theory, the system's time responses under the Kern County earthquake with the PGA of 0.5 g are plotted in Figure 7. The frequency spectra of the 1st floor's peak RD and the top floor's peak AA in different damper configurations for the Kern County earthquake (PGA = 0.5 g) are shown in Figure 8a,b, respectively.

It can be seen from Tables 1, 2, 3, and 4 that the damping efficiency of AVTLd is higher than that of AUTLd for peak and RMS values of the RD of the first floor and the AA of the top floor. In addition, the RMS liquid column displacement w of AVTLd is lower than that of AUTLd. The difference in the RMS value of control force between AVTLd and AUTLd is insignificant. Simulation results in Figures 2, 3, 4, 5, and 6 and Tables 1, 2, 3, and 4 clearly show the advantages of VTLCD over UTLCD in general and AVTLd over AUTLd in particular, especially in earthquakes with high and average PGAs (0.7 and 0.5 g).

It is noted that the investigation results in [34, 35] have shown that VTLCD is suitable for earthquakes with high PGAs. However, this conclusion has only been verified for one DOF structures under harmonic load with the linearized damping of VTLCD and UTLCD. The results of this study also confirm the above conclusion; the validations have been extended to the multidegree-of-freedom model under seismic loads with nonlinear VTLCD and UTLCD.

5. Conclusions

This study is an extension of our recent publication on vibration reduction for earthquake-resistant structures using passive VTLCD and UTLCD. The publication's structural model, optimization criteria, and simulation scenarios are adopted for the investigations of hybrid control using VTLCD and UTLCD in this work. The main results of this work are summarized as follows.

- The primary innovation is the move from passive control to hybrid control for VTLCD. In addition to the advantages of VTLCD over UTLCD demonstrated in the previous research for the passive control problem, the vibration reduction effectiveness of VTLCD continues to be investigated in the context of the hybrid control problem in this work.
- The simplest version of the HAC is used to calculate the control force on the structure's first floor to reduce the complexity and calculation time of the control action.
- The structure-VTLCD system with the control force applied to the structure's first floor provides significantly better structural vibration reduction efficiency than the system using UTLCD in all investigated earthquakes with different PGAs.

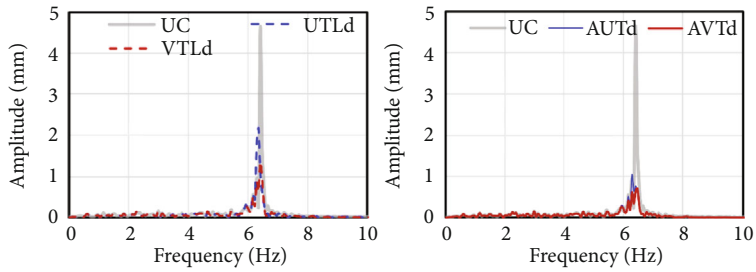

(a) Peak RD of the 1st floor, Kern County—0.5g

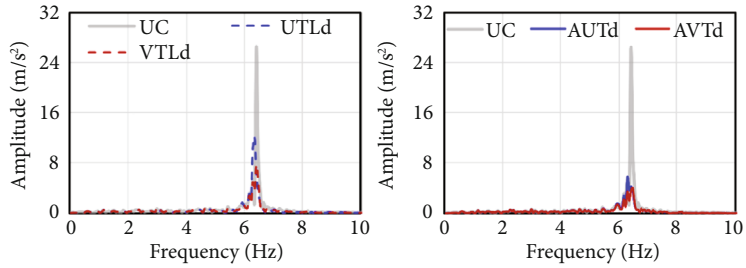

(b) Peak AA of the top floor, Kern County—0.5g

Figure 8: Frequency spectra of the 1st floor's peak RD and the top floor's peak AA, Kern County—0.5 g.

- When the PGA of the investigated earthquakes increases, this efficiency increases, demonstrating the advantage of VTLCD even in the case of hybrid control.

The investigation results in this study can be extended to many exciting topics, for example, optimizing VTLCD with variable cross-sections, evaluating the trade-off level between objectives, designing a multi-VTLCD model for multiple-degrees-of-freedom systems, and studying improved forms of VTLCDs in passive, active, or hybrid controls. The main shortcoming of this paper is the lack of real-world experimental results on VTLCD configurations. Therefore, conducting experimental studies for VTLCD is necessary to confirm its practical performance in controlling structural vibrations. Although this study focuses on a relatively stiff five-story structure, future work will aim to evaluate the performance of VTLCDs across a wider range of structural types, including more flexible or stiff systems. Such an extension would help generalize the conclusions and better understand the applicability of VTLCDs to short-period structures, particularly in tuning strategies and practical implementation challenges.

Data Availability Statement

Data is available on request from the authors.

Conflicts of Interest

The authors declare no conflicts of interest.

Funding

This study was supported by the Hanoi University of Science and Technology (HUST) (T2023-PC-007).

References

[1] A. Mousaad, "Vibration Control of Buildings Using Magnetorheological Damper: A New Control Algorithm," *Journal of Engineering* 2013, no. 1 (2013): 596078, https://doi.org/10.1155/2013/596078.

[2] M. Jafari and A. Alipour, "Methodologies to Mitigate Wind-Induced Vibration of Tall Buildings: A State-of-the-Art Review," *Journal of Building Engineering* 33 (2021): 101582, https://doi.org/10.1016/j.jobe.2020.101582.

[3] F. Yang, R. Sedaghati, and E. Esmailzadeh, "Vibration Suppression of Structures Using Tuned Mass Damper Technology: A State-of-the-Art Review," *Journal of Vibration and Control* 28, no. 7-8 (2022): 812–836, https://doi.org/10.1177/1077546320984305.

[4] T. Konar and A. Ghosh, "A Review on Various Configurations of the Passive Tuned Liquid Damper," *Journal of Vibration and Control* 29, no. 9-10 (2023): 1945–1980, https://doi.org/10.1177/10775463221074077.

[5] M. J. Hochrainer, "Tuned Liquid Column Damper for Structural Control," *Acta Mechanica* 175, no. 1-4 (2005): 57–76, https://doi.org/10.1007/s00707-004-0193-z.

[6] L. E. Mackriell, K. C. S. Kwok, and B. Samali, "Critical Mode Control of a Wind-Loaded Tall Building Using an Active Tuned Mass Damper," *Engineering Structures* 19, no. 10 (1997): 834–842, https://doi.org/10.1016/S0141-0296(97)00172-7.

[7] M.-Y. Liu, W.-L. Chiang, J.-H. Hwang, and C.-R. Chu, "Wind-Induced Vibration of High-Rise Building With Tuned Mass Damper Including Soil–Structure Interaction," *Journal of Wind Engineering and Industrial Aerodynamics* 96, no. 6-7 (2008): 1092–1102, https://doi.org/10.1016/j.jweia.2007.06.034.

[8] S. Elias and V. Matsagar, "Distributed Multiple Tuned Mass Dampers for Wind Vibration Response Control of High-Rise Building," *Journal of Engineering* 2014, no. 1 (2014): 198719, https://doi.org/10.1155/2014/198719.

[9] A.-P. Wang, R.-F. Fung, and S.-C. Huang, "Dynamic Analysis of a Tall Building With a Tuned-Mass-Damper Device

Subjected to Earthquake Excitations," *Journal of Sound and Vibration* 244, no. 1 (2001): 123–136, https://doi.org/10.1006/jsvi.2000.3480.

[10] N.-A. Tran, V.-B. Bui, and H.-L. Bui, "Optimization of Multi-TMD Using BCMO for Building Models Subjected to Earthquake," in *Advances in Engineering Research and Application: Proceedings of the International Conference on Engineering Research and Applications* (ICERA, 2023), 1–6.

[11] N. Debnath, S. K. Deb, and A. Dutta, "Multi-Modal Vibration Control of Truss Bridges With Tuned Mass Dampers Under General Loading," *Journal of Vibration and Control* 22, no. 20 (2016): 4121–4140, https://doi.org/10.1177/1077546315571172.

[12] B. Mokrani, Z. Tian, D. Alaluf, F. Meng, and A. Preumont, "Passive Damping of Suspension Bridges Using Multi-Degree of Freedom Tuned Mass Dampers," *Engineering Structures* 153 (2017): 749–756, https://doi.org/10.1016/j.engstruct.2017.10.028.

[13] O. Araz and V. Kahya, "Optimization of Non-Traditional Tuned Mass Damper for Damped Structures Under Harmonic Excitation," *Uludağ Üniversitesi Mühendislik Fakültesi Dergisi* 26, no. 3 (2021): 1021–1034, https://doi.org/10.17482/uumfd.878114.

[14] O. Araz, "Effect of Basic Parameters Defining Principal Soil-Structure Interaction on Seismic Control of Structures Equipped With Optimum Tuned Mass Damper," *Soil Dynamics and Earthquake Engineering* 189 (2025): 109085, https://doi.org/10.1016/j.soildyn.2024.109085.

[15] V. Kahya and O. Araz, "A Sequential Approach Based Design of Multiple Tuned Mass Dampers Under Harmonic Excitation," *Sigma Journal of Engineering and Natural Sciences* 37, no. 1 (2019): 225–239.

[16] O. Araz, "Optimum Three-Element Tuned Mass Damper for Damped Main Structures Under Ground Acceleration," *El-Cezeri* 8, no. 3 (2021): 1264–1271, https://doi.org/10.31202/ecjse.913901.

[17] Y. Tamura, K. Fujii, T. Ohtsuki, T. Wakahara, and R. Kohsaka, "Effectiveness of Tuned Liquid Dampers Under Wind Excitation," *Engineering Structures* 17, no. 9 (1995): 609–621, https://doi.org/10.1016/0141-0296(95)00031-2.

[18] Y. Tamura, "Application of Damping Devices to Suppress Wind-Induced Responses of Buildings," *Journal of Wind Engineering and Industrial Aerodynamics* 74-76 (1998): 49–72, https://doi.org/10.1016/S0167-6105(98)00006-3.

[19] P. Banerji, M. Murudi, A. H. Shah, and N. Popplewell, "Tuned Liquid Dampers for Controlling Earthquake Response of Structures," *Earthquake Engineering & Structural Dynamics* 29, no. 5 (2000): 587–602, https://doi.org/10.1002/(SICI)1096-9845(200005)29:5%3C587::AID-EQE926%3E3.0.CO;2-I.

[20] Y. Xin, G. Chen, and M. Lou, "Seismic Response Control With Density-Variable Tuned Liquid Dampers," *Earthquake Engineering and Engineering Vibration* 8, no. 4 (2009): 537–546, https://doi.org/10.1007/s11803-009-9111-7.

[21] T. Konar and A. Ghosh, "Development of a Novel Tuned Liquid Damper With Floating Base for Converting Deep Tanks Into Effective Vibration Control Devices," *Advances in Structural Engineering* 24, no. 2 (2021): 401–407, https://doi.org/10.1177/1369433220953539.

[22] T. Konar, A. Das, and A. Ghosh, "Enhancing Tunability of Liquid Storage Tanks to Function as Deep Tuned Liquid Dampers by Use of a Submerged Stretched Membrane," *Structural Control and Health Monitoring* 29, no. 12 (2022): e3109, https://doi.org/10.1002/stc.3109.

[23] A. Das and T. Konar, "Design and Optimization of Roof-Top Fire Water Tanks as Compliant Deep Tank Dampers-Inerter for Seismic Protection of Multi-Storeyed Buildings," *Journal of Building Engineering* 80 (2023): 107957, https://doi.org/10.1016/j.jobe.2023.107957.

[24] T. Konar and A. D. Ghosh, "Adaptive Design of an Overhead Water Tank as Dynamic Vibration Absorber for Buildings by Use of a Stiffness-Varying Support Arrangement," *Journal of Vibration Engineering & Technologies* 11, no. 3 (2023): 827–843, https://doi.org/10.1007/s42417-022-00611-y.

[25] K. Swaroop, "Semi-Active Tuned Liquid Column Dampers for Vibration Control of Structures," *Engineering Structures* 23, no. 11 (2001): 1469–1479, https://doi.org/10.1016/S0141-0296(01)00047-5.

[26] B. Samali, E. Mayol, K. C. S. Kwok, A. Mack, and P. Hitchcock, "Vibration Control of the Wind-Excited 76-Story Benchmark Building by Liquid Column Vibration Absorbers," *Journal of Engineering Mechanics* 130, no. 4 (2004): 478–485, https://doi.org/10.1061/(ASCE)0733-9399(2004)130:4(478).

[27] A. Ghosh and B. Basu, "Seismic Vibration Control of Short Period Structures Using the Liquid Column Damper," *Engineering Structures* 26, no. 13 (2004): 1905–1913, https://doi.org/10.1016/j.engstruct.2004.07.001.

[28] E. Sonmez, S. Nagarajaiah, C. Sun, and B. Basu, "A Study on Semi-Active Tuned Liquid Column Dampers (sTLCDs) for Structural Response Reduction Under Random Excitations," *Journal of Sound and Vibration* 362 (2016): 1–15, https://doi.org/10.1016/j.jsv.2015.09.020.

[29] F. Zhu, J.-T. Wang, F. Jin, and L. Li-Qiao, "Real-Time Hybrid Simulation of Full-Scale Tuned Liquid Column Dampers to Control Multi-Order Modal Responses of Structures," *Engineering Structures* 138 (2017): 74–90, https://doi.org/10.1016/j.engstruct.2017.02.004.

[30] V. D. La and C. Adam, "General on-off Damping Controller for Semi-Active Tuned Liquid Column Damper," *Journal of Vibration and Control* 24, no. 23 (2018): 5487–5501, https://doi.org/10.1177/1077546316648080.

[31] Q. H. Cao, "Vibration Control of Structures by an Upgraded Tuned Liquid Column Damper," *Journal of Engineering Mechanics* 147, no. 9 (2021): 04021052, https://doi.org/10.1061/(ASCE)EM.1943-7889.0001965.

[32] H.-L. Bui, N.-A. Tran, and H. Q. Cao, "Active Control Based on Hedge-Algebras Theory of Seismic-Excited Buildings With Upgraded Tuned Liquid Column Damper," *Journal of Engineering Mechanics* 149, no. 1 (2023): 04022091, https://doi.org/10.1061/JENMDT.EMENG-6821.

[33] H. Q. Cao, N.-A. Tran, and H.-L. Bui, "Hedge-Algebras-Based Hybrid Control of Earthquake-Induced Buildings Using Upgraded Tuned Liquid Column Dampers," *Soil Dynamics and Earthquake Engineering* 182 (2024): 108728, https://doi.org/10.1016/j.soildyn.2024.108728.

[34] H. Gao, K. C. S. Kwok, and B. Samali, "Optimization of Tuned Liquid Column Dampers," *Engineering Structures* 19, no. 6 (1997): 476–486, https://doi.org/10.1016/S0141-0296(96)00099-5.

[35] H. Gao, K. S. C. Kwok, and B. Samali, "Characteristics of Multiple Tuned Liquid Column Dampers in Suppressing Structural Vibration," *Engineering Structures* 21, no. 4 (1999): 316–331, https://doi.org/10.1016/S0141-0296(97)00183-1.

[36] M. Shadman and A. Akbarpour, "Comparative Study of Utilizing a New Type V-Shaped Tuned Liquid Column Damper and U-Shaped Tuned Liquid Column Damper in Floating Wind Turbines," in *International Conference on Offshore Mechanics*

and Arctic Engineering (American Society of Mechanical Engineers, 2012).

[37] N.-A. Tran, H.-L. Bui, and Q.-H. Cao, "U-Shaped and V-Shaped Tuned Liquid Column Dampers in Vibration Reduction of Earthquake-Induced Buildings: A Comparative Study," *Structure* 65 (2024): 106669, https://doi.org/10.1016/j.istruc.2024.106669.

[38] V.-B. Bui, T.-T. Mac, and H.-L. Bui, "Design Optimization Considering the Stability Constraint of the Hedge-Algebras-Based Controller for Building Structures Subjected to Seismic Excitations," *Proceedings of the Institution of Mechanical Engineers, Part I: Journal of Systems and Control Engineering* 237, no. 10 (2023): 1822–1837, https://doi.org/10.1177/09596518231171960.

[39] V.-T. Nguyen, N.-A. Tran, and H.-L. Bui, "Application of HA Theory-Based Controller and BCMO Algorithm in Passive and Hybrid Control of Nonlinear Building Structures With TLCD Subjected to Earthquake," *Proceedings of the Institution of Mechanical Engineers, Part C: Journal of Mechanical Engineering Science* 239, no. 14 (2025): 5313–5325, https://doi.org/10.1177/09544062251327549.

[40] H.-L. Bui, T.-D. Nguyen, and V.-D. Le, "Optimal Design of Hedge-Algebras-Based Controller for Active Suspension Systems With Parameter Uncertainty," in *International Conference on Advances in Information and Communication Technology* (Springer, 2023).

[41] T.-T. Mac, T.-D. Nguyen, H.-L. Bui, and N.-A. Tran, "Optimal Design of Hedge-Algebras–Based Controller for Vibration Control of Vehicle Suspension Systems," *Proceedings of the Institution of Mechanical Engineers, Part I: Journal of Systems and Control Engineering* 238, no. 4 (2023): 755–776, https://doi.org/10.1177/09596518231196900.

[42] S.-T. Nguyen, T.-T. Mac, and H.-L. Bui, "Motion Control of a Mobile Robot Using the Hedge–Algebras-Based Controller," *Journal of Robotics* 2023, 13https://doi.org/10.1155/2023/6613293.

[43] T.-D. Nguyen, S.-T. Nguyen, T. T. Mac, and H.-L. Bui, "Trajectory Tracking of Mobile Robots Using Hedge-Agebras-Based Controllers," *Intelligent Service Robotics* 17, no. 4 (2024): 793–814, https://doi.org/10.1007/s11370-024-00529-2.

[44] F. Y. Cheng, H. Jiang, and K. Lou, *Smart Structures: Innovative Systems for Seismic Response Control* (CRC Press, 2008).

[45] K. S. Ashok and K. S. Arvind, *Numerical Methods for Ordinary Differential Equations With Programs* (Alpha Science, 2018).

[46] N. C. Ho and W. Wechler, "Hedge Algebras: An Algebraic Approach to Structure of Sets of Linguistic Truth Values," *Fuzzy Sets and Systems* 35, no. 3 (1990): 281–293, https://doi.org/10.1016/0165-0114(90)90002-N.

[47] N. C. Ho and W. Wechler, "Extended Hedge Algebras and Their Application to Fuzzy Logic," *Fuzzy Sets and Systems* 52, no. 3 (1992): 259–281, https://doi.org/10.1016/0165-0114(92)90237-X.

[48] N. C. Ho and N. Van Long, "A Topological Completion of Refined Hedge Algebras and a Model of Fuzziness of Linguistic Terms and Hedges," *Fuzzy Sets and Systems* 158, no. 4 (2007): 436–451, https://doi.org/10.1016/j.fss.2006.09.013.

[49] T.-D. Nguyen and H.-L. Bui, "General Optimization Procedure of the Hedge-Algebras Controller for Controlling Dynamic Systems," *Artificial Intelligence Review* 56, no. 3 (2023): 2749–2784, https://doi.org/10.1007/s10462-022-10242-0.

[50] A. H. Nayfeh and B. Balachandran, *Applied Nonlinear Dynamics: Analytical, Computational, and Experimental Methods* (John Wiley & Sons, 2008).

[51] X.-T. Nguyen, H.-H. Hoang, H.-L. Bui, and T.-T. Mac, "An Elman Neural Network Approach in Active Control for Building Vibration Under Earthquake Excitation," *Frontiers of Structural and Civil Engineering* 19, no. 1 (2025): 60–75, https://doi.org/10.1007/s11709-025-1156-9.

[52] N.-A. Tran, V.-B. Hoang, H.-L. Bui, and H. Q. Cao, "Upgraded Double Tuned Mass Dampers for Vibration Control of Structures Under Earthquakes," *Computers & Structures* 310 (2025): 107700, https://doi.org/10.1016/j.compstruc.2025.107700.

[53] N.-A. Tran and H.-L. Bui, "Rolling Tuned Mass Damper for Vibration Control of Building Structures Subjected to Earthquakes: A Comparative Study," *Soil Dynamics and Earthquake Engineering* 194 (2025): 109376, https://doi.org/10.1016/j.soildyn.2025.109376.